Probing RNA Hairpins with Cobalt(III)hexammine and Electrospray Ionization Mass Spectrometry

Jason W. Kieltyka and Christine S. Chow
Department of Chemistry, Wayne State University, Detroit, Michigan, USA

In this work, electrospray ionization mass spectrometry (ESI MS) was employed to study the interactions of cobalt(III) hexammine, $Co(NH_3)_6^{3+}$, with five RNA hairpins representing the 790 loop of 16S ribosomal RNA and 1920 loop of 23S ribosomal RNA. The RNAs varied in mismatch identity (G·U versus A·C) and level of base modification (pseudouridine versus uridine). $Co(NH_3)_6^{3+}$ binding was observed with the four RNA hairpins that contained a G·U wobble pair in the stem region. ESI MS revealed 1:1 and 1:2 complex formation with all RNAs. Weaker binding was observed with the fifth RNA hairpin that contained an A·C wobble pair in the stem region. The effects of pH on $Co(NH_3)_6^{3+}$ binding were also examined. (J Am Soc Mass Spectrom 2006, 17, 1376–1382) © 2006 American Society for Mass Spectrometry

Electrospray ionization mass spectrometry (ESI MS) can be used to detect noncovalent interactions, and there are a number of examples in the literature for nucleic acid-ligand interactions (reviewed in [1, 2]). Several advantages of using MS over other biochemical techniques include speed of analysis, high sensitivity, absence of radioactive or fluorescent labels, ability to analyze mixtures, and coupling with LC (liquid chromatography) techniques. In this work, we report on the utility of ESI MS to study noncovalent interactions between RNA and transition-metal complexes. Ligand binding to five RNA hairpins with varying sequences or sites of modification was investigated.

The first objective was to determine if cobalt(III)hexammine, $Co(NH_3)_6^{3+}$, could discriminate between G·U and A·C wobble pairs (Figure 1). Biological studies on 16S ribosomal RNA (rRNA) revealed that G·U is a functional substitute for A·C in certain sequence contexts [3]. Studies by Kieft and Tinoco on the P5b stem loop of a group I intron ribozyme indicated that $Co(NH_3)_6^{3+}$ binding occurred in the major groove of a series of tandem G·U mismatches and the complex formed hydrogen bonds with both Gs [4]. Additional contacts were observed with neighboring Gs, and while the carbonyls of the Us did not participate in hydrogen bonding, they likely added to the negative surface of the binding pocket [4]. Gdaniec et al. studied an iron regulatory element in ferritin mRNA and observed $Co(NH_3)_6^{3+}$ binding in a pocket consisting of a GC base pair, a bulge, and a dynamic G·U wobble pair, and suggested that $Co(NH_3)_6^{3+}$ binding may stabilize the structure around the G·U wobble pair [5].

Magnesium(II) plays an important role in RNA structural motifs [6]. RNAs often contain specific Mg(II) binding sites in which the interactions range from hydrogen bonds with the bases or phosphate backbone to direct covalent bonds with oxygens of the phosphate backbone [7, 8]. Studying the interactions of $Mg(H_2O)_6^{2+}$ with RNA is often limited to specific methods such as X-ray crystallography [9]. Cowan [10] proposed that $Co(NH_3)_6^{3+}$ could serve as a probe of $Mg(H_2O)_6^{2+}$ binding sites, because both ions have similar ionic radii and geometries, and interact with RNA in a similar manner (Figure 1) [4, 5, 11–12]. More specifically, $Co(NH_3)_6^{3+}$ can substitute for the $Mg(H_2O)_6^{2+}$ outer coordination sphere contacts with RNA [4, 10, 13]. NMR spectroscopy has typically been the method of choice to study $Co(NH_3)_6^{3+}$ interactions with RNA, but it is time-consuming and requires large quantities of sample. In addition, high concentrations of Mg(II) lead to line broadening in NMR spectra [14]. Extensive adduction of Mg(II) cations with RNA is often observed in mass spectrometry experiments. The goal of this study was to use ESI MS to detect $Co(NH_3)_6^{3+}$ binding to RNAs containing G·U and A·C wobble pairs as well as modified bases such as pseudouridine (Ψ) and 3-methylpseudouridine ($m^3\Psi$) (Figure 1). Differences in $Co(NH_3)_6^{3+}$ binding to the various RNAs may reflect subtle structural variations between mismatches or modified sites as well as potential differences in $Mg(H_2O)_6^{2+}$ interactions.

Two families of rRNAs were studied. The first was

Published online August 9, 2006
Address reprint requests to Professor C. S. Chow, Department of Chemistry, Wayne State University, 5101 Cass Avenue, Detroit, MI 48202, USA. E-mail: csc@chem.wayne.edu

1044-0305/06/$32.00
doi:10.1016/j.jasms.2006.07.006

Received March 14, 2006
Revised July 3, 2006
Accepted July 6, 2006

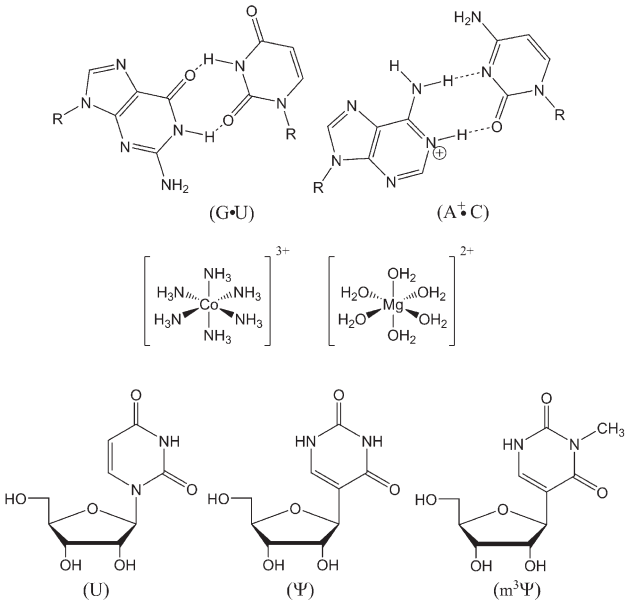

Figure 1. The top panel depicts the G·U and A^+·C wobble pairs. R indicates the ribose sugar. The middle panel depicts the geometries of $Co(NH_3)_6^{3+}$ and $Mg(H_2O)_6^{2+}$, and the bottom panel shows the structures of uridine (U), pseudouridine (Ψ), and 3-methylpseudouridine ($m^3\Psi$).

modeled after the 790 loop (positions 786 to 796 of *E. coli* 16S rRNA, Figure 2) [3]. This region of rRNA is important because it is located in the small ribosomal subunit of all organisms and plays a role in protein synthesis through inter-subunit interactions, initiation factor 3 binding, and tRNA binding [15–18]. Extensive genetic and NMR studies have been carried out on the 790 loop, and mutations to this key hairpin resulted in diminished ribosome function [3, 15, 16, 19]. The two 790 loops used in this study have the same general secondary structure, but differ by a single base·base mismatch at positions 787 and 795. An A·C to G·U mutation at positions 787·795 was not deleterious to ribosome function [3]. The 790 GU loop contains a G_{787}·U_{795} mismatch, whereas the 790 AC loop contains an A_{787}·C_{795} mismatch. The second family was modeled after the 1920 loop (positions 1906 to 1924 of *E. coli* 23S rRNA, Figure 2). This region is important because it is located in the large ribosomal subunit of all organisms and forms an inter-subunit bridge (referred to as bridge B2a, which connects the decoding region to the peptidyl transferase center) [20, 21] and contacts tRNAs, the decoding region [22], and the previously mentioned 790 loop [23, 24]. The three 1920 loop RNAs used in this study are as follows: 1920 UUU contains Us at positions 1911, 1915, and 1917, whereas 1920 ΨΨΨ contains Ψs at those positions [25]. The 1920 $\Psi m^3\Psi\Psi$ RNA contains Ψs at positions 1911 and 1917 and an $m^3\Psi$ at position 1915 [26]. Our goal was to first study $Co(NH_3)_6^{3+}$ binding to these smaller, well-defined RNA hairpins before initiating experiments on the entire ribosome.

Materials and Methods

Chemicals

All reagents were purchased as either molecular biology grade or the highest purity grade available, and they were obtained from Acros Organics (Morris Plains, NJ), Fisher Scientific Company (Fair Lawn, NJ), or Sigma-Aldrich Company (St. Louis, MO) unless otherwise stated. Ultrapure deionized 18 MΩ water was obtained from a Millipore Biocel water filtration system (Bedford, MA).

RNA Preparation and Purification

The oligonucleotides 5′-GGCGGUUAGAUAUCGCC-3′ (790 GU loop), 5′-GGCGAUUAGAUACCGCC-3′ (790 AC loop), 5′-GGCCGUAACUAUAACGGUC-3′ (1920 UUU loop), 5′-GGCCGΨAACΨAΨAACGGUC-3′ (1920 ΨΨΨ loop), and 5′-GGCCGΨAAC($m^3\Psi$)-AΨAACGGUC-3′ (1920 $\Psi m^3\Psi\Psi$ loop) were chemically synthesized at Dharmacon, Inc. (Lafayette, CO) on a 1.0 μmol scale via the phosphoramidite method [27]. 3-Methylpseudouridine ($m^3\Psi$) was synthesized in our laboratory, converted into its phosphoramidite form, and then sent to Dharmacon, Inc. for incorporation into the 1920 $\Psi m^3\Psi\Psi$ loop [28]. The crude RNAs were received as the 2′-*O*-ACE protected species and deprotected by dissolving in a 100 mM TEMED-acetic acid solution (**N**,**N**,**N**′,**N**′,-tetramethylethylenediamine, pH 3.8, followed by incubation at 60 °C for 30 min [27]. The RNAs were then dried in a speed-vac evaporator and reconstituted in water. The RNAs were purified via HPLC with a Waters XTerra MS (Milford, MA) C_{18} 2.5 micron, 10 mm × 50 mm column and a gradient of 20% to 57.5% buffer B in 15 min at 4.5

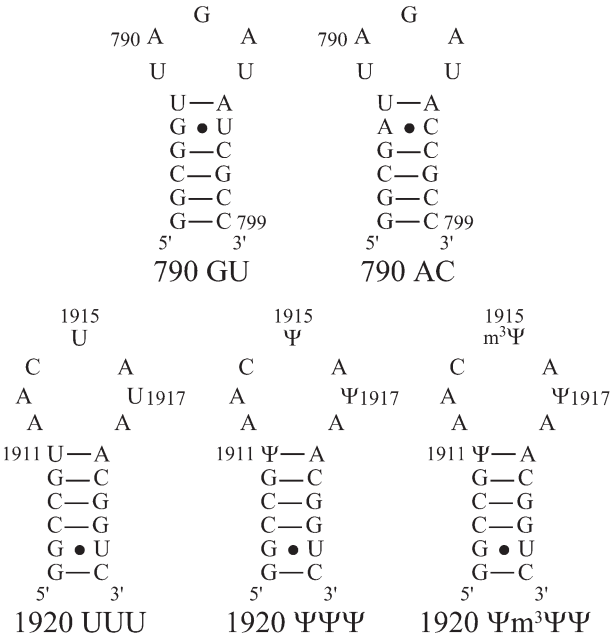

Figure 2. The RNA hairpins used in this study are illustrated. The numbering is based on the complete *E. coli* 16S [44] and 23S [45] secondary structures.

mL/min at room temperature (Buffer A: 5% acetonitrile in 0.1 M triethylammonium acetate, pH 7; Buffer B: 15% acetonitrile in 0.1 M triethylammonium acetate, pH 7). The RNA fractions were detected at 260 nm and collected manually.

Following HPLC purification, the RNAs were dried and twice precipitated from either 8 M ammonium acetate, pH 7.2, or 4 M ammonium acetate, pH 5.3. The RNAs were then dried, reconstituted in water, and stored at −20 °C. The RNAs were renatured in 30 μL aliquots (200 μM) containing 90 to 100 mM ammonium acetate (pH 5.3 or 7.2) by incubation at 90 °C for 15 min, followed by slow cooling to room temperature. RNA concentrations were calculated using Beer's Law and $A_{260\ nm}$ measurements. Extinction coefficients (ε) were calculated using the nearest-neighbor method [29]; 168,300, 167,500, and 188,860 $L \cdot mol^{-1} \cdot cm^{-1}$ for the 790 GU, 790 AC, and 1920 UUU loops, respectively. The ε value obtained for the 1920 UUU loop was also used for the 1920 ΨΨΨ and $\Psi m^3\Psi\Psi$ loops.

Solution and ESI MS Conditions

Solutions for ESI MS analysis had final concentrations of 4 to 5.9 μM RNA, 21 mM ammonium acetate (pH 7.2 or 5.3), 2 to 35% 2-propanol, and a range of $Co(NH_3)_6^{3+}$ concentrations. The samples were mixed and incubated for 15 min before ESI MS analysis. Alternatively, samples were prepared 24 h in advance of MS analysis. No difference was observed between the two methods except that RNA samples at pH 5.3 showed signs of depurination after long incubation times. To test for nonspecific RNA–ligand interactions, an RNA:ligand ratio of 1:1 was maintained while ammonium acetate (pH 7.2) concentrations varied from 10 to 150 mM. ESI MS samples of RNA were infused at 6 μL/min via a Harvard II syringe pump and analyzed in the negative ionization mode on a Quattro LC tandem quadrupole mass spectrometer (Micromass, Manchester, UK). Spectra were acquired over the range 600 to 2000 *m/z*. Typically, 80 to 110 scans were summed to obtain representative spectra. The error resulting from replicate measurements at a given concentration was 12% maximally. The Quattro LC settings were as follows: capillary voltage 2500 V, cone voltage 40 to 50 V, extractor cone voltage 2 V, RF lens voltage 0.6 V, nebulizer gas flow ~90 L/h, desolvation gas flow ~400 L/h, source block temperature 100 °C, and desolvation temperature 100 to 120 °C.

To compare $Co(NH_3)_6^{3+}$ binding to the various RNAs, the fraction of the 1:1 and 1:2 complexes were calculated. We assumed that the relative abundances of the multiply charged peaks were representative of solution concentrations, and that the RNA and RNA − $Co(NH_3)_6^{3+}$ complexes had the same ionization efficiencies [30–32]. Thus, the concentrations of the free RNA, 1:1, and 1:2 complexes were assumed to be proportional to the summed peak areas of the charge states from the free RNA, 1:1, and 1:2 complexes, respectively. The fraction of the free RNA, 1:1, or 1:2 complex was determined by dividing the sum of the peak areas for the complex of interest by the total peak area ($j = \frac{\sum Aj}{\sum A_{total}}$), where j is the fraction of the species of interest and A is the peak area. This conversion allowed for a comparison of solutions containing the same [RNA]:[$Co(NH_3)_6^{3+}$] ratios.

Results and Discussion

$Co(NH_3)_6^{3+}$ Binding to the 790 Loops at pH 7.2

Our first set of experiments was carried out on the 790 loops from *E. coli* 16S rRNA. The binding of $Co(NH_3)_6^{3+}$ to the 790 GU loop was examined at pH 7.2 over a range of concentrations. Figure 3 compares the mass spectra obtained for this system as the concentration of $Co(NH_3)_6^{3+}$ was varied from 0 to 9.3 μM. Four charge states (3- through 6-) of the free RNA were observed (data summarized in Table 1). All four charge states exhibited the formation of the 1:1 RNA-$Co(NH_3)_6^{3+}$

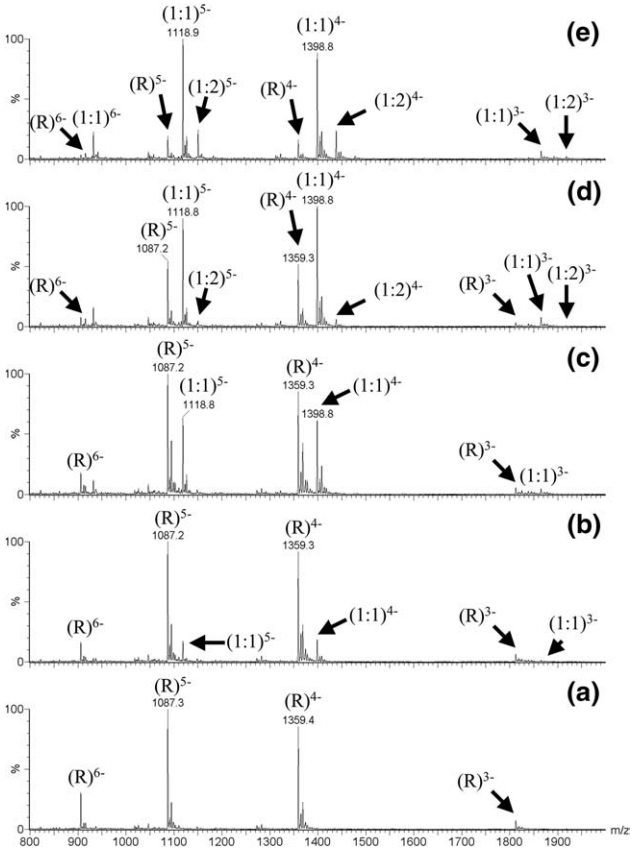

Figure 3. Negative ion ESI MS spectra of reaction mixtures containing 5.9 μM 790 GU loop RNA, 22 mM ammonium acetate, pH 7.2, 25% 2-propanol, and (**a**) 0.0, (**b**) 0.5, (**c**) 1.9, (**d**) 3.3, and (**e**) 9.3 μM $Co(NH_3)_6^{3+}$. Molar ratios of RNA:$Co(NH_3)_6^{3+}$ were (**a**) 1:0, (**b**) 1:0.1, (**c**) 1:0.3, (**d**) 1:0.6, and (**e**) 1:1.6. Free RNA charge states are labeled as $(R)^{n-}$, and 1:1 and 1:2 complexes are labeled as $(1:1)^{n-}$ and $(1:2)^{n-}$, respectively, where n indicates the charge state.

Table 1. The m/z values are listed for the charge states of the RNA and RNA − $Co(NH_3)_6^{3+}$ complexes

	790 Loops		1920 Loops		
Species	GU	AC	UUU	ψψψ	ψm³ψψ
$[RNA - 6H^+]^{6-}$	906	903	1009	1009	1011
$[RNA - 5H^+]^{5-}$	1087	1084	1211	1211	1214
$[RNA - 4H^+]^{4-}$	1359	1355	1514	1514	1518
$[RNA - 3H^+]^{3-}$	1813	1807	—	—	—
$[RNA + Co(NH_3)_6^{3+} - 9H^+]^{6-}$	932	nd	nd	nd	nd
$[RNA + Co(NH_3)_6^{3+} - 8H^+]^{5-}$	1119	1116	1243	1243	1246
$[RNA + Co(NH_3)_6^{3+} - 7H^+]^{4-}$	1399	1395	1554	1554	1557
$[RNA + Co(NH_3)_6^{3+} - 6H^+]^{3-}$	1867	1860	—	—	—
$[RNA + 2Co(NH_3)_6^{3+} - 12H^+]^{6-}$	nd	nd	nd	nd	nd
$[RNA + 2Co(NH_3)_6^{3+} - 11H^+]^{5-}$	1151	1147	1274	1274	1277
$[RNA + 2Co(NH_3)_6^{3+} - 10H^+]^{4-}$	1438	1434	1593	1593	1597
$[RNA + 2Co(NH_3)_6^{3+} - 9H^+]^{3-}$	1920	1912	—	—	—

nd indicates species not detected.
— indicates charge states outside the scanned m/z range.

species (Table 1). The most intense charge states were 5- and 4-, which accounted for roughly 85% of the total peak area of each spectrum. A second bound $Co(NH_3)_6^{3+}$ was also identified (Table 1). The fraction of the 1:1 complex steadily increased up to 0.7 (at which point saturation was reached) at 9 μM $Co(NH_3)_6^{3+}$ (the fraction of the 1:2 complex was 0.20 at this point) (Figure 3). The 1:2 complex reached saturation at 120 μM $Co(NH_3)_6^{3+}$ (the fraction of 1:2 complex at saturation was 0.4, data not shown). As shown in Figure 3d, the ratios of free 790 GU RNA to 1:1 complex at 3 μM $Co(NH_3)_6^{3+}$ were 0.5:1 and 0.6:1 for the 4- and 5- charge states, respectively. Similar behavior was observed for the 1:2 complex. Since ~50% of the $Co(NH_3)_6^{3+}$ was bound (1:1) at 1.9 μM, the apparent dissociation constant is estimated to be ~2 μM for the first $Co(NH_3)_6^{3+}$ binding site. For the second $Co(NH_3)_6^{3+}$ binding site, the apparent dissociation constant is estimated to be >10 μM at pH 7.2.

To determine if a nonspecific binding component existed between the 790 GU loop and $Co(NH_3)_6^{3+}$, the RNA and $Co(NH_3)_6^{3+}$ concentrations were held constant at a 1:1.1 ratio and the ammonium acetate concentration was increased from 10 to 120 mM. If the $Co(NH_3)_6^{3+}$ binding was governed mainly by electrostatic interactions, then the amount of 1:1 and/or 1:2 species would be expected to diminish as the ammonium acetate concentration increased. At higher concentrations (60–120 mM) of ammonium acetate, the fraction of 1:1 complex remained steady (0.6–0.7, data not shown), whereas the fraction of 1:2 complex steadily decreased from 0.4 to 0.1 (at 10 and 120 mM ammonium acetate, respectively). The signal-to-noise ratio became progressively worse with increasing amounts of ammonium acetate, with an upper limit of ~120 mM. Therefore, the observed $Co(NH_3)_6^{3+}$ binding to the 790 GU loop appears to be a combination of specific and nonspecific interactions.

The results for $Co(NH_3)_6^{3+}$ binding to the 790 AC loop differed from those obtained with the 790 GU loop. Figure 4 shows more free RNA under similar conditions as those for the 790 GU loop (for example, compare Figures 3 and 4, panels d and e). Since ~50% of $Co(NH_3)_6^{3+}$ is bound (1:1) at 2.5 μM (Figure 4, panel d), the apparent dissocia-

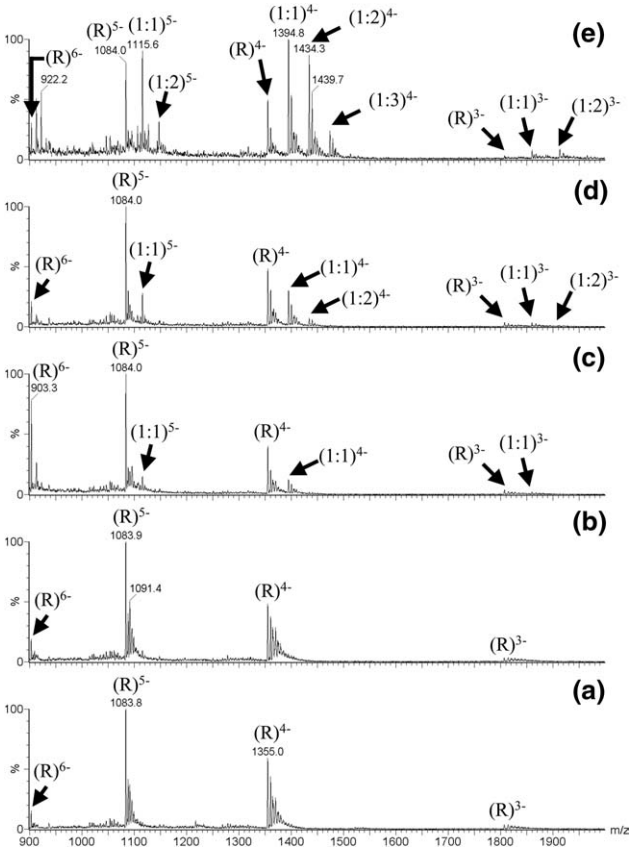

Figure 4. Negative ion ESI MS spectra of reaction mixtures containing 4.0 μM 790 AC loop RNA, 22 mM ammonium acetate, pH 7.2, 25% 2-propanol, and (**a**) 0.0, (**b**) 0.3, (**c**) 1.4, (**d**) 2.5, and (**e**) 6.5 μM $Co(NH_3)_6^{3+}$. Molar ratios of RNA:$Co(NH_3)_6^{3+}$ were (**a**) 1:0, (**b**) 1:0.1, (**c**) 1:0.3, (**d**) 1:0.6, and (**e**) 1:1.6. Free RNA charge states are labeled as $(R)^{n-}$, and 1:1 and 1:2 complexes are labeled as $(1:1)^{n-}$ and $(1:2)^{n-}$, respectively, where n indicates the charge state.

tion constant at pH 7.2 is estimated to be ~4 μM. The free RNA charge states remained the most abundant species until an RNA:ligand molar ratio of 1:0.6 was reached. At higher ligand concentrations, both 1:2 and 1:3 complexes were observed. The fractions of the 1:1, 1:2, and 1:3 complexes increased to 0.4, 0.3, and 0.1 (saturation points), respectively (Figure 4). For comparison, the 1:1 complex reached saturation at approximately the same concentration of $Co(NH_3)_6^{3+}$ (5–10 μM) for the 790 GU and AC loops; however, the fractions of bound ligand were 0.7 and 0.4, respectively. These differences could be accounted for by the fact that the cobalt complex appeared to have a greater number of binding sites on the 790 AC loop. Overall, there was an approximate 2-fold higher affinity of $Co(NH_3)_6^{3+}$ for the primary site (1:1 complex) on the 790 GU loop compared to the 790 AC loop, but lower affinity for the secondary sites. Thus, clearly the single base mismatch difference between 790 GU and AC loop RNAs leads to altered $Co(NH_3)_6^{3+}$ binding. NMR studies by Lee et al. indicates similar global folds for the 790 GU and AC loops [3]. Therefore, the difference in binding modes by $Co(NH_3)_6^{3+}$ may reflect subtle variations in the structures of the 790 GU versus 790 AC loop RNAs. The increase in number of $Co(NH_3)_6^{3+}$ binding sites on the 790 AC loop indicated that the structural change or possible change in electrostatics due to altered base composition extends beyond the mismatch site. The 790 AC loop spectra exhibited similar charge state distributions as the 790 GU loop. A 2- to 3-fold difference in the relative abundance of free RNA between the 3- and 5- charge states was also observed.

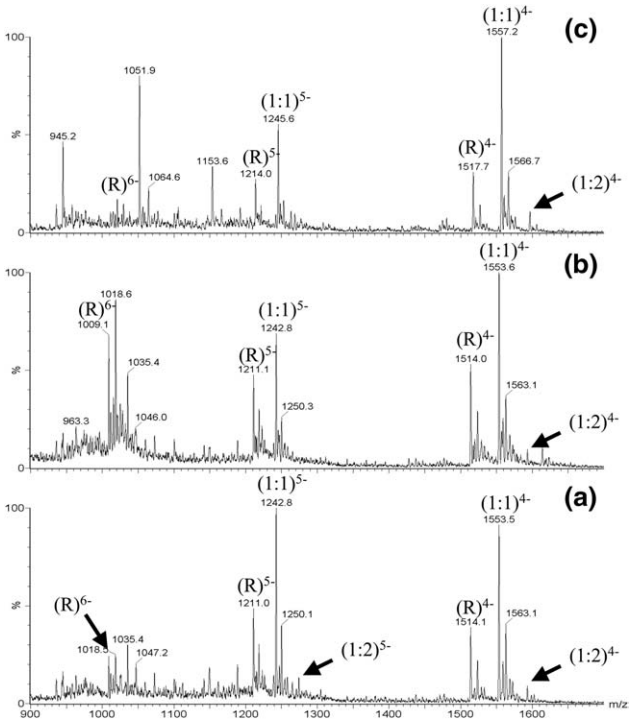

Figure 5. Negative ion ESI MS spectra of reaction mixtures containing 4.0 μM RNA, 22 mM ammonium acetate, pH 7.2, 25% 2-propanol, and 0.5 μM $Co(NH_3)_6^{3+}$ for (**a**) 1920 UUU loop, (**b**) 1920 ΨΨΨ loop, and (**c**) 1920 Ψm^{3}ΨΨ loop. The molar ratios of RNA:$Co(NH_3)_6^{3+}$ were 1:0.5. Free RNA charge states are labeled as $(R)^{n-}$, and 1:1 and 1:2 complexes are labeled as $(1:1)^{n-}$ and $(1:2)^{n-}$, respectively, where n indicates the charge state.

$Co(NH_3)_6^{3+}$ Binding to the 1920 Loops at pH 7.2

Figure 5 shows the ESI MS analyses of 1:0.5 RNA: $Co(NH_3)_6^{3+}$ solutions (pH 7.2) of the 1920 loops. The results were similar to those with the 790 GU loop. The most abundant ions at *m/z* 1243 and 1246 are assigned to the 1:1 complexes. These three hairpins all have a G·U wobble pair located in the stem region, but differ in their loop compositions (U, Ψ, or m^{3}Ψ at 1911, 1915, and 1917). These results suggest that the common motif, the G·U wobble pair, in the 1920 stem region could be the binding site of $Co(NH_3)_6^{3+}$. These results are consistent with previous NMR studies that revealed $Co(NH_3)_6^{3+}$ binding to a G·U mismatch [5]. For the 1920 UUU, 1920 ΨΨΨ, and 1920 Ψm^{3}ΨΨ loops, saturation was reached at ~2 μM $Co(NH_3)_6^{3+}$ for the 1:1 complex with a maximum fraction bound of 0.6. The dissociation constants were estimated to be <0.5 μM because more than 50% of the 1:1 complex formed at 0.5 μM $Co(NH_3)_6^{3+}$. The apparent dissociation constants are about 4-fold lower for the 1920 loops compared to the 790 GU loop, suggesting that the sequence surrounding the G·U mismatch site also influences the binding of $Co(NH_3)_6^{3+}$. Subtle differences in the fraction of the 1:2 complex with $Co(NH_3)_6^{3+}$ and the 1920 loop RNAs indicate that a second binding site might occur in the loop region, which is the location of changes in the RNA composition (modified versus unmodified nucleotides).

$Co(NH_3)_6^{3+}$ Binding to the 790 Loops at pH 5.3

Literature reports suggested that G·U and protonated A·C wobble pairs are isostructural [33, 34]. As indicated in Figure 1, the A·C wobble pair is stabilized at lower pH due to protonation of the A residue (pK_a ~5.5). $Co(NH_3)_6^{3+}$ titrations and ESI MS studies were carried out at pH 5.3 on the 790 loop hairpins. In a previous study, lowering the pH from 7.0 to 5.3 resulted in an increase in the thermodynamic stability of the 790 AC loop, whereas pH changes did not affect the 790 GU loop stability [3]. Lee et al. also suggested that the protonated A·C wobble pair was structurally isomorphous to the G·U wobble pair (within the context of the 790 loops), and that the overall structures of the two hairpins were also isomorphous as determined by NMR spectroscopy [3].

ESI MS data for $Co(NH_3)_6^{3+}$ binding to the 790 loops at pH 5.3 and pH 7.2 are compared in Figure 6 (for ease of comparison, only the data for the lower concentrations of $Co(NH_3)_6^{3+}$ are shown). At pH 5.3 (Figure 6 panels a and c), only the 3-, 4-, and 5- charge states were observed. The 6- ion was only observed at pH 7.2 (panels b and d). This effect is consistent with the work of Cheng et al. in which a lowering of the pH of a DNA solution caused the envelope of charge states to narrow and shift towards lower charge states, and resulted in simpler spectra [35]. If the RNA was stored overnight at

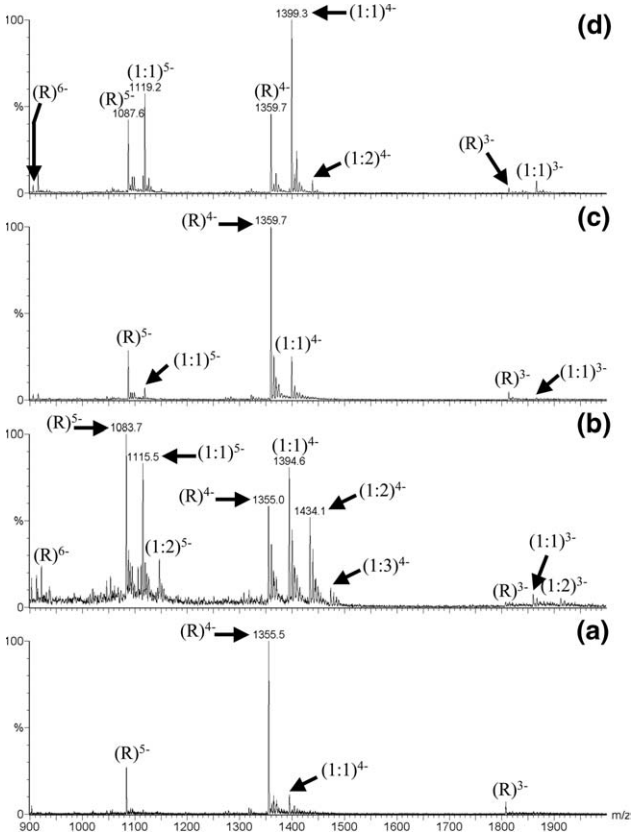

Figure 6. Negative ion ESI MS spectra of reaction mixtures containing equimolar amounts of $Co(NH_3)_6^{3+}$ and (**a**) the 790 AC loop RNA, pH 5.3, (**b**) the 790 AC loop RNA, pH 7.2, (**c**) the 790 GU loop RNA, pH 5.3, and (**d**) the 790 GU loop RNA, pH 7.2. All solutions contained 22 mM ammonium acetate, 25% 2-propanol, 4 μM RNA, and 4 μM $Co(NH_3)_6^{3+}$. Free RNA charge states are labeled as $(R)^{n-}$ and 1:1 complexes are labeled as $(1:1)^{n-}$, where n indicates the charge state.

room-temperature in pH 5.3 buffer, a significant amount of depurination was observed, specifically loss of G from the hairpin (10% of the total RNA). Less binding by $Co(NH_3)_6^{3+}$ at pH 5.3 was observed with both RNAs (panels a and c). The spectra shown in Figure 6 indicated a 68 and 74% decrease of 1:1 complex formation for the 790 GU (panel c) and AC (panel a) loops, respectively. For the 790 GU loop, the fraction of 1:1 complex at saturation decreased from 0.7 to 0.5 as the pH was lowered from 7.2 to 5.3, and saturation was not reached until 30 μM $Co(NH_3)_6^{3+}$. This result indicated an approximate 3-fold decrease in binding affinity and a corresponding decrease in specificity at the lower pH since more 1:2 complex was observed at higher $Co(NH_3)_6^{3+}$ concentrations (data not shown). For the 790 AC loop, the fraction of 1:1 complex at saturation remained the same (0.4) as the pH was lowered, but saturation was not reached until ~150 μM $Co(NH_3)_6^{3+}$. This result indicated an approximate 30-fold decrease in binding affinity at the lower pH.

The shift in the charge state distribution upon lowering the pH suggests that the 790 loops have been protonated at the lower pH, which is logical for the 790 AC loop [3]. Studies of DNA hairpins by Guo et al. [36] suggested that ammonium ions are transferred to base nitrogens in the gas-phase (as was previously determined by Green-Church and Limbach for monodeoxynucleotides and mononucleotides [37]), which suggested that the 790 GU loop can also be protonated. More ring nitrogens are accessible in unpaired DNA/RNA bases. If ligand binding does occur at the mismatch site, then protonation of that site (790 A^+·C) could account for a substantial decrease in $Co(NH_3)_6^{3+}$ binding at pH 5.3. Indeed, the 790 GU loop showed a less significant decrease in $Co(NH_3)_6^{3+}$ binding. The ~3-fold decrease in binding affinity of $Co(NH_3)_6^{3+}$ for the 790 GU hairpin at lower pH indicated that a base in the hairpin is likely protonated. Either loop or stem protonation could lead to unfavorable interactions with $Co(NH_3)_6^{3+}$ due to charge repulsions. Metal binding directly at the mismatch site would be affected more significantly by a protonated 790 AC loop (i.e., A^+·C) compared to the 790 GU loop (i.e., G·U), as indicated by the ~30-fold decrease in binding affinity of $Co(NH_3)_6^{3+}$ for the 790 AC hairpin at lower pH.

Are the ESI MS Results Reflective of Solution-Phase Behavior?

One important question is whether the ESI MS results obtained in this study are reflective of the solution-phase behavior of RNA and $Co(NH_3)_6^{3+}$. Studies by Gidden et al. indicated that as DNA is dehydrated during the electrospray process, it converts from B-form to a metastable A-form-type helix, before converting to a globular form [38, 39]. Molecular dynamics studies indicated that A-form helices were the most stable helical form in the gas phase [38, 39]. To assess the solution binding, the 790 GU loop–$Co(NH_3)_6^{3+}$ interaction was studied using isothermal titration calorimetry (ITC). ITC is thought to be one of the most reliable and high-precision methods to quantitate ligand-receptor interactions, and it has successfully been used to investigate nucleic acid–metal complex interactions [40–42]. ITC and ESI MS studies were performed under the same buffer conditions, allowing a direct comparison. These preliminary studies revealed that in 22 mM ammonium acetate, pH 7.2, the 790 GU loop contained a relatively strong (~0.2 μM K_d) and a relatively weak (~90 μM K_d) $Co(NH_3)_6^{3+}$ binding site, which is in agreement with the data presented here. The complete ITC results will be presented elsewhere.

Conclusions

In this study, noncovalent interactions between RNA and transition-metal complexes were observed using ESI MS. Our studies with $Co(NH_3)_6^{3+}$ and five model hairpins indicated binding of $Co(NH_3)_6^{3+}$ to RNAs that contain G·U wobble pairs. The four RNAs that contained G·U wobble pairs exhibited higher fractions of

1:1 complex formation (between 0.6 and 0.7) than the RNA that had the G·U replaced with an A·C wobble pair (0.2). Thus, discrimination of $Co(NH_3)_6^{3+}$ binding to RNAs of different sequences (G·U versus A·C) was observed. A lack of significant discrimination between the modified 1920 RNAs suggested that $Co(NH_3)_6^{3+}$ binding is not strongly influenced by these modified nucleotides. The 1:2 complex formation was minimal for all five RNAs. Subtle differences in the fractions of 1:2 complex for the 1920 loops suggested, however, that the modified nucleotides are affecting the structure or electrostatics at the second $Co(NH_3)_6^{3+}$ binding site.

ESI MS appears to be a viable technique to investigate metal complex–RNA interactions [43]. This technique could prove to be quite valuable for understanding the binding behavior of divalent metal ions, such as Mg(II). Since metal ions play important roles in most biological systems, particularly in the case of RNA and ribozymes, ESI MS can provide information about their binding affinities and possible sites of interaction.

Acknowledgments

The authors thank Professors Mary Rodgers and Pat Limbach for helpful discussions, and Dr. Lew Hryhorczuk and Dr. Brian Shay for instrument training. The ITC studies were carried out by Professor Takashi Morii and Tetsuya Hasegawa (Kyoto University). JWK acknowledges Wayne State University for a Summer Dissertation Fellowship. This work was supported by the NIH (GM54632).

References

1. Hofstadler, S. A.; Griffey, R. H. Analysis of Noncovalent Complexes of DNA and RNA by Mass Spectrometry. *Chem. Rev.* **2001**, *101*, 377–390.
2. Beck, J. L.; Colgave, M. L.; Ralph, S. F.; Sheil, M. M. Electrospray Ionization Mass Spectrometry of Oligonucleotide Complexes with Drugs, Metals, and Proteins. *Mass Spectrom. Rev.* **2001**, *20*, 61–87.
3. Lee, K.; Varma, S.; SantaLucia, J., Jr.; Cunningham, P. R. *In vivo* Determination of RNA Structure–Function Relationships: Analysis of the 790 Loop in Ribosomal RNA. *J. Mol. Biol.* **1997**, *269*, 732–743.
4. Kieft, J. S.; Tinoco, I., Jr. Solution Structure of a Metal-Binding Site in the Major Groove of RNA Complexed with Cobalt(III) Hexammine. *Structure* **1997**, *5*, 713–721.
5. Gdaniec, Z.; Sierzputowska-Gracz, H.; Theil, E. C. Iron Regulatory Element and Internal Loop/Bulge Structure for Ferritin mRNA Studied by Cobalt(III) Hexammine Binding, Molecular Modeling, and NMR Spectroscopy. *Biochemistry* **1998**, *37*, 1505–1512.
6. Pyle, A. M. Metal Ions in the Structure and Function of RNA. *J. Biol. Inorg. Chem.* **2002**, *7*, 679–690.
7. Cowan, J. A. *Inorganic Biochemistry: An Introduction*, 2nd ed.; Wiley-VCH: New York, NY, 1997; p 274.
8. Lippard, S. J.; Berg, J. M. Principles of Bioinorganic Chemistry; University Science Books: Mill Valley, CA, 1994; p 194
9. Holbrook, S. R.; Sussman, J. L.; Warrant, R. W.; Church, G. M.; Kim, S.-H. RNA-Ligand Interactions: (I) Magnesium Binding Sites in Yeast $tRNA^{Phe}$. *Nucleic Acids Res.* **1977**, *4*, 2811–2820.
10. Cowan, J. A. Metallobiochemistry of RNA. $Co(NH_3)_6^{3+}$ as a Probe for Mg^{2+} (aq) Binding Sites. *J. Inorg. Biochem.* **1993**, *49*, 171–175.
11. Schmitz, M.; Tinoco, I., Jr. Solution Structure and Metal-Ion Binding of the P4 Element from Bacterial RNase P RNA. *RNA* **2000**, *6*, 1212–1225.
12. Rudisser, S.; Tinoco, I., Jr. Solution Structure of Cobalt(III)Hexammine Complexed to the GAAA Tetraloop, and Metal-ion Binding to G·A Mismatches. *J. Mol. Biol.* **2000**, *295*, 1211–1223.
13. Kim, S.; Cowan, J. A. Inert Cobalt Complexes as Mechanistic Probes of the Biochemistry of Magnesium Co-factors. Application to Topoisomerase I. *Inorg. Chem.* **1992**, *31*, 3495–3496.
14. Gonzalez, R. L., Jr.; Tinoco, I., Jr. Solution Structure and Thermodynamics of a Divalent Metal Ion Binding Site in an RNA Pseudoknot. *J. Mol. Biol.* **1999**, *289*, 1267–1282.
15. Herr, W.; Chapman, N. M.; Noller, H. F. Mechanism of Ribosomal Subunit Association: Discrimination of Specific Sites in 16 S RNA Essential for Association Activity. *J. Mol. Biol.* **1979**, *130*, 433–449.
16. Tapprich, W. E.; Goss, D. J.; Dahlberg, A. E. Mutation at Position 791 in *Escherichia coli* 16S Ribosomal RNA Affects Processes Involved in the Initiation of Protein Synthesis. *Proc. Natl. Acad. Sci. U.S.A.* **1989**, *86*, 4927–4931.
17. Moazed, D.; Noller, H. F. Transfer RNA Shields Specific Nucleotides in 16S Ribosomal RNA from Attack by Chemical Probes. *Cell* **1986**, *47*, 985–994.
18. Moazed, D.; Samaha, R. R.; Gualerzi, C.; Noller, H. F. Specific Protection of 16S rRNA by Translational Initiation Factors. *J. Mol. Biol.* **1995**, *248*, 207–210.
19. Santer, M.; Bennett-Guerrero, E.; Byahatti, S.; Czarnecki, S.; O'Connell, D.; Meyer, M.; Khoury, J.; Cheng, X.; Schwartz, I.; McLaughlin, J. Base Changes at Position 792 of *Escherichia coli* 16S rRNA Affect Assembly of 70S Ribosomes. *Proc. Natl. Acad. Sci. U.S.A.* **1990**, *87*, 3700–3704.
20. Schuwirth, B. S.; Borovinskaya, M. A.; Hau, C. W.; Zhang, W.; Vila-Sanjurjo, A.; Holton, J. M.; Cate, J. H. D. Structures of the Bacterial Ribosome at 3.5 Å Resolution. *Science* **2005**, *310*, 827–834.
21. Yusupov, M. M.; Yusupova, G. Z.; Baucom, A.; Liebeman, K.; Earnest, T. N.; Cate, J. H.; Noller, H. F. Crystal Structure of the Ribosome at 5.5 Å Resolution. *Science* **2001**, *292*, 883–896.
22. Mitchell, P.; Osswald, M.; Brimacombe, R. Identification of Intermolecular RNA Cross-Links at the Subunit Interface of the *Escherichia coli* Ribosome. *Biochemistry* **1992**, *31*, 3004–3011.
23. Joeseph, S.; Weiser, B.; Noller, H. F. Mapping the Inside of the Ribosome with an RNA Helical Ruler. *Science* **1997**, *278*, 1093–1098.
24. Merryman, C.; Moazed, D.; Daubresse, G.; Noller, H. F. Nucleotides in 23S rRNA Protected by the Association of 30S and 50S Ribosomal Subunits. *J. Mol. Biol.* **1999**, *285*, 107–113.
25. Ofengand, J.; Bakin, A. Mapping to Nucleotide Resolution of Pseudouridine Residues in Large Subunit Ribosomal RNAs from Representative Eukaryotes, Prokaryotes, Archaebacteria, Mitochondria, and Chloroplasts. *J. Mol. Biol.* **1997**, *266*, 246–268.
26. Kowalak, J. A.; Pomerantz, S. C.; Crain, P. F.; McCloskey, J. A. A Novel Method for the Determination of Post-transcriptional Modification in RNA by Mass Spectrometry. *Nucleic Acids Res.* **1993**, *21*, 4577–4585.
27. Scaringe, S. A.; Wincott, F. E.; Caruthers, M. H. Novel RNA Synthesis Method Using 5′-*O*-Silyl-2′-*O*-Orthoester Protecting Groups. *J. Am. Chem. Soc.* **1998**, *120*, 11820–11821.
28. Chui, H. M.-P.; Desaulniers, J.-P.; Scaringe, S. A.; Chow, C. S. Synthesis of Helix 69 of *Escherichia coli* 23S rRNA Containing Its Natural Modified Nucleosides, m^3-Psi and Psi. *J. Org. Chem.* **2002**, *67*, 8847–8854.
29. Richards, E. G. Use of Tables in Calculating Absorption, Optical Rotary Dispersion, and Circular Dichroism of Polyribonucleotides. Fasman, G. D., Ed.; In Handbook of Biochemistry and Molecular Biology: Nucleic Acids; CRC Press: Cleveland, OH, 1975; pp 569–599.
30. Loo, J. A. Studying Noncovalent Protein Complexes by Electrospray Ionization Mass Spectrometry. *Mass Spectrom. Rev.* **1997**, *16*, 1–23.
31. Sannes-Lowery, K. A.; Griffey, R. H.; Hofstadler, S. A. Measuring Dissociation Constants of RNA and Aminoglycoside Antibiotics by Electrospray Ionization Mass Spectrometry. *Anal. Biochem.* **2000**, *280*, 264–271.
32. Bligh, S. W. A.; Haley, T.; Lowe, P. N. Measurement of Dissociation Constants of Inhibitors Binding to Src SH2 Domain Protein by Noncovalent Electrospray Ionization Mass Spectrometry. *J. Mol. Recognit.* **2003**, *16*, 139–148.
33. Brown, T.; Leonard, G. A.; Booth, E. D.; Kneale, G Influence of pH on the Conformation and Stability of Mismatch Base-Pairs in DNA. *J. Mol. Biol.* **1990**, *212*, 437–440.
34. Hunter, W. N.; Brown, T.; Anand, N. N.; Kennard, O. Structure of an Adenine-Cytosine Base Pair in DNA and Its Implications for Mismatch Repair. *Nature* **1986**, *320*, 552–555.
35. Cheng, X.; Gale, D. C.; Udseth, H. R.; Smith, R. D. Charge State Reduction of Oligonucleotide Negative Ions from Electrospray Ionization. *Anal. Chem.* **1995**, *67*, 586–593.
36. Guo, X.; Bruist, M. F.; Davis, D. L.; Bentzley, C. M. Secondary Structural Characterization of Oligonucleotide Strands using Electrospray Ionization Mass Spectrometry. *Nucleic Acids Res.* **2005**, *33*, 3659–3666.
37. Green-Church, K. B.; Limbach, P. A. Mononucleotide Gas-Phase Proton. Affinities as Determined by the Kinetic Method. *J. Am. Soc. Mass Spectrom.* **2000**, *11*, 24–32.
38. Gidden, J.; Baker, E. S.; Ferzoco, A.; Bowers, M. T. Structural Motifs of DNA Complexes in the Gas Phase. *Int. J. Mass Spectrom.* **2005**, *240*, 183–193.
39. Gidden, J.; Ferzoco, A.; Baker, E. S.; Bowers, M. T. Duplex Formation and the Onset of Helicity in Poly $d(CG)_n$ Oligonucleotides in a Solvent-Free Environment. *J. Am. Chem. Soc.* **2004**, *126*, 15132–15140.
40. Mundoma, C.; Greenbaum, N. L. Sequestering of Eu(III) by a GAAA RNA Tetraloop. *J. Am. Chem. Soc.* **2002**, *124*, 3525–3532.
41. Xu, H.; Liang, Y.; Zhang, P.; Du, F.; Zhou, B.-R.; Wu, J.; Liu, J.-H.; Liu, Z.-G.; Ji, L.-N. Biophysical Studies of a Ruthenium(II) Polypyridyl Complex Binding to DNA and RNA Prove that Nucleic Acid Structure has Significant Effects on Binding Behaviors. *J. Biol. Inorg. Chem.* **2005**, *10*, 529–538.
42. Hammann, C.; Cooper, A.; Lilley, D. M. Thermodynamics of Ion-Induced RNA Folding in the Hammerhead Ribozyme: An Isothermal Titration Calorimetric Study. *Biochemistry* **2001**, *40*, 1423–1429.
43. Urathamakul, T.; Beck, J. L.; Sheil, M. M.; Aldrich-Wright, J. R.; Ralph, S. F. A Mass Spectrometric Investigation of Noncovalent Interactions Between Ruthenium Complexes and DNA. *Dalton Trans.* **2004**, *17*, 2683–2690.
44. Gutell, R. R. Collection of Small Subunit (16S- and 16S-like) Ribosomal RNA Structures: 1994. *Nucleic Acids Res.* **1994**, *22*, 3502–3507.
45. Gutell, R. R.; Gray, M. W.; Schnare, M. N. A Compilation of Large Subunit (23S and 23S-like) Ribosomal RNA Structures: 1993. *Nucleic Acids Res.* **1993**, *21*, 3055–3074.